PNAS

Supplementary Information for

NOS2 and S-nitrosothiol signaling induces DNA hypomethylation and LINE-1 retrotransposon expression.

Christopher H. Switzer[1*], Hyun-Ju Cho[1], Thomas R. Eykyn[2], Paul Lavender[3] and Philip Eaton[1*]

[1]William Harvey Research Institute, Barts & The London School of Medicine and Dentistry, Queen Mary University of London, London, United Kingdom. [2]School of Biomedical Engineering & Imaging Sciences, King's College London, St. Thomas' Hospital, London, UK. [3]AsthmaUK Centre in Allergic Mechanisms of Asthma, School of Immunology and Microbial Science, King's College London, Guy's Hospital, London, United Kingdom

* Christopher H. Switzer or Philip Eaton
Email: c.switzer@qmul.ac.uk or p.eaton@qmul.ac.uk

This PDF file includes:

> Figures S1 to S7
> Tables S1 to S6
> Legends for Datasets S1
> SI References

Other supplementary materials for this manuscript include the following:

> Datasets S1
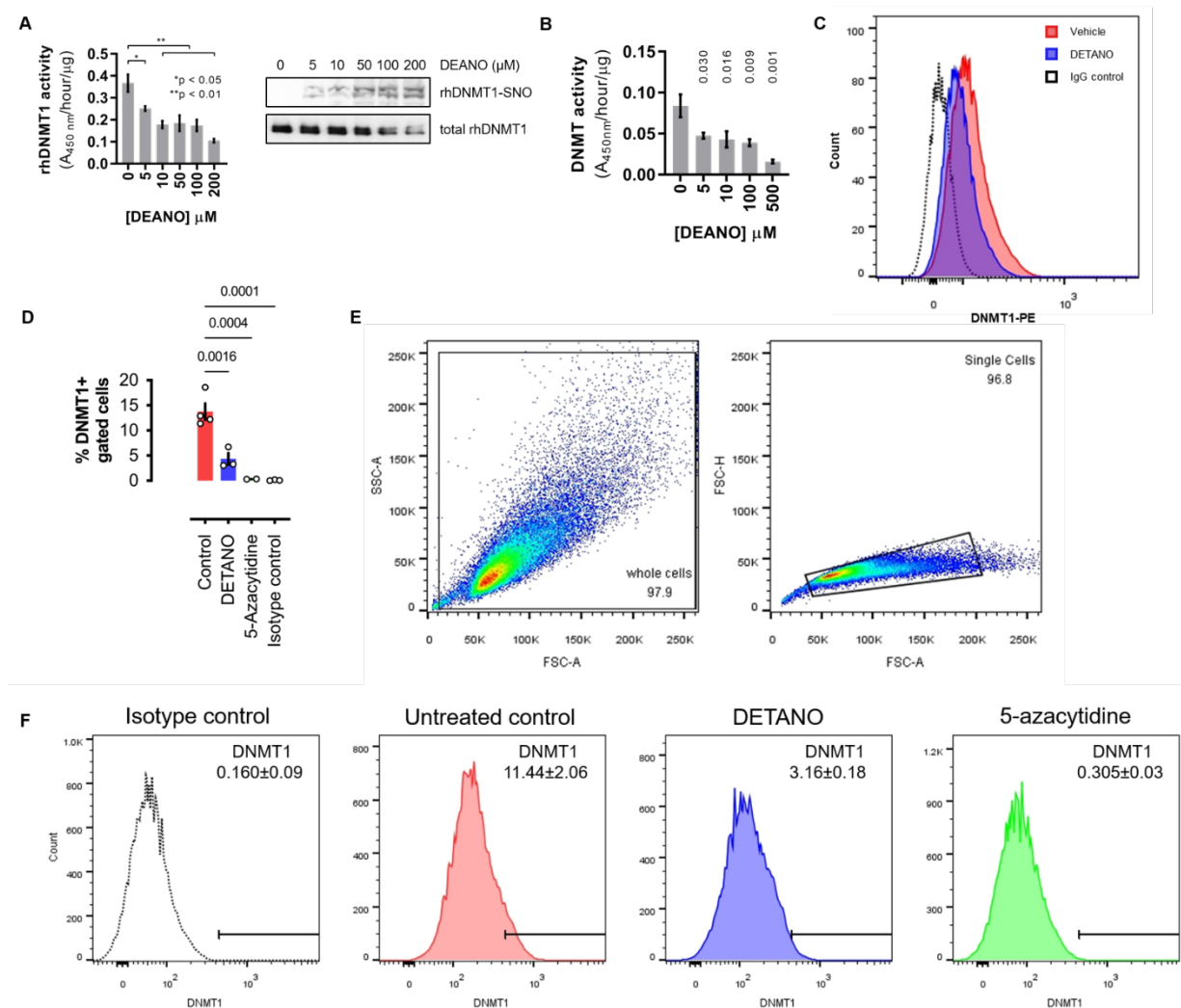
Fig. S1. NOS2 induces LINE-1 expression and DNA damage.
A Recombinant human DNMT1 activity treated with DEANO compared to vehicle (10 mM NaOH) treatment. Graph shows mean activity (±sem; n = 3). Significance was calculated by one-way ANOVA with Dunnett's multiple comparisons test. Immunoblot showing DNMT1-SNO PTM and total DNMT1 from rhDNMT1 reacted with DEANO (100 μM) or vehicle for 30 minutes. **B** Total cytosine methyltransferase activity from isolated nuclei treated with DEANO. Graph shows mean activity (±sem; n = 3). Statistical significance from control was determined by one-way ANOVA with Dunnett's multiple comparison test and calculated P values are displayed above bars. **C** Cytometric histogram of DNMT1 expression in MDA-MB-231 cells treated with DETANO or vehicle and compared isotype control stained cells. **D** Graph depicting the mean percentages of gated DNMT1-positive MDA-MB-231 cells after indicated treatment (±sem; n = 2-4). Gating strategy is shown in E and F. Statistical significance from control was determined by one-way ANOVA with Dunnett's multiple comparisons test. **E** Gating strategy for obtaining whole (left) and single cells (right) for DNMT1-PE analysis. **F** Histogram plots of untreated control MDA-MB-231, DETANO- and 5-azacytidine-treated cells stained with DNMT1-PE and IgG-PE isotype stained control cells. DNMT1-PE gating was established from the isotype control as shown by the horizontal bar.**G** Cell viability of cell lines treated with DETANO for 48 hours. Data shown are mean values (±sem; n = 3). **H** DNMT3A protein expression in MDA-MB-231 cells treated with DETANO (300 μM) or 5-azacytidine (5 μM) for 48 hours. **I** Principle component analysis of Illumina MethylationEPIC bead chip array. **J** Immunoblot of relative DNMT1 protein expression in MDA-MB-231 cells treated with vehicle or DETANO and 1 μM ODQ (soluble guanylyl cyclase inhibitor). Graph represents mean

normalized DNMT1 expression (±sem; n = 4). Significance was calculated by two-way ANOVA with Sidak multiple comparisons test. **K** Immunoblot of relative DNMT1 protein expression in MDA-MB-231 cells treated with DETANO or 8-pCPT-cGMP for 24 hours and compared to untreated cells. Graph represents mean normalized DNMT1 expression (±sem; n = 4). Statistical significance from control was determined by one-way ANOVA with Dunnett's multiple comparison test and calculated P values are displayed above bars. **L** Immunoblot of relative TET2 protein expression in MDA-MB-231 cells cultured with DETANO or vehicle for 48 hours. Graph depicts mean normalized DNMT1expression levels (±sem; n = 3). Significance was calculated by two-tailed, unpaired t test. **M** TET activity from MDA-MB-231 cells treated with vehicle or DETANO for 48 hours. Mean activity is shown (±sem; n = 4). Significance was calculated by two-tailed, unpaired t test. **N** 5-hydroxymethylcytosine content from MDA-MB-231 cells treated with vehicle or DETANO for 48 hours. Data is shown as percent of total cytosine measured and mean percentages are displayed (±sem; n = 5). Significance was calculated by two-tailed, unpaired t test. **O** Immunoblot of relative DNMT1 and Myc-tag expression in MDA-MB-231 cells transiently transfected with empty vector or Myc-DNMT1 expression plasmid and then cultured with DETANO or vehicle for 48 hours. **P** 5-methylcytosine content (β) from cells described in N (β = 5-methylcytosine/total cytosine). Graph represents mean 5mC content (±sem; n = 4). Significance was calculated by two-way ANOVA with Sidak multiple comparisons test. **Q** Representative immunoblot of NOS2 and DNMT1 protein expression in NOS2-GFP transfected MDA-MB-231 and MCF7 cell lines.
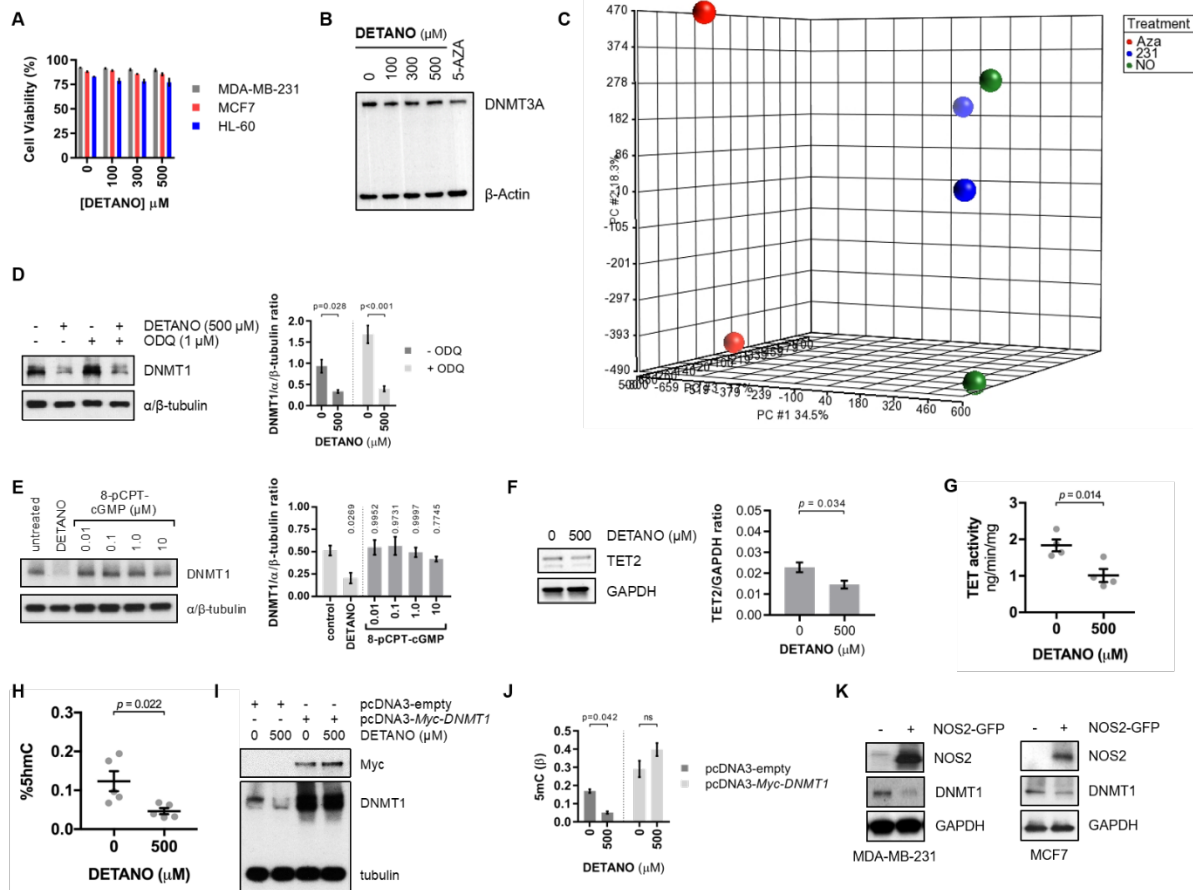
Fig. S2. Non-canonical S-nitrosothiol (SNO) signaling induces passive DNA demethylation.
A Cell viability of cell lines treated with DETANO for 48 hours. Data shown are mean values (±sem; n = 3). **B** Relative DNMT3A protein expression in MDA-MB-231 cells treted with DETANO or 5-azacytidine for 48 hours. **C** Principle component analysis of Illumina MethylationEPIC bead chip array. **D** Immunoblot of relative DNMT1 protein expression in MDA-MB-231 cells treated with vehicle or DETANO and 1 μM ODQ (soluble guanylyl cyclase inhibitor). Graph represents mean normalized DNMT1 expression (±sem; n = 4). Significance was calculated by two-way ANOVA with Sidak multiple comparisons test. **E** Immunoblot of relative DNMT1 protein expression in MDA-MB-231 cells treated with DETANO or 8-pCPT-cGMP for 24 hours and compared to untreated cells. Graph represents mean normalized DNMT1 expression (±sem; n = 4). Statistical significance from control was determined by one-way ANOVA with Dunnett's multiple comparison test and calculated P values are displayed above bars. **F** Immunoblot of relative TET2 protein expression in MDA-MB-231 cells cultured with DETANO or vehicle for 48 hours. Graph depicts mean normalized DNMT1expression levels (±sem; n = 3). Significance was calculated by two-tailed, unpaired t test. **G** TET activity from MDA-MB-231 cells treated with vehicle or DETANO for 48 hours. Mean activity is shown (±sem; n = 4). Significance was calculated by two-tailed, unpaired t test. **H** 5-hydroxymethylcytosine content from MDA-MB-231 cells treated with vehicle or DETANO for 48 hours. Data is shown as percent of total cytosine measured and mean percentages are displayed (±sem; n = 5). Significance was calculated by two-tailed, unpaired t test. **I** Immunoblot of relative DNMT1 and Myc-tag expression in MDA-MB-231 cells transiently transfected with empty vector or Myc-DNMT1 expression plasmid and then cultured with DETANO or vehicle for 48 hours. **J** 5-methylcytosine content (β) from cells described in N (β = 5-methylcytosine/total cytosine). Graph represents mean 5mC content (±sem; n = 4). Significance was calculated by two-way ANOVA with Sidak multiple comparisons test. **K** Immunoblots of NOS2 and DNMT1 protein expression in MCF7 and MDA-MB-231 cells 48 hours after transfection with or without NOS-GFP plasmid.

4
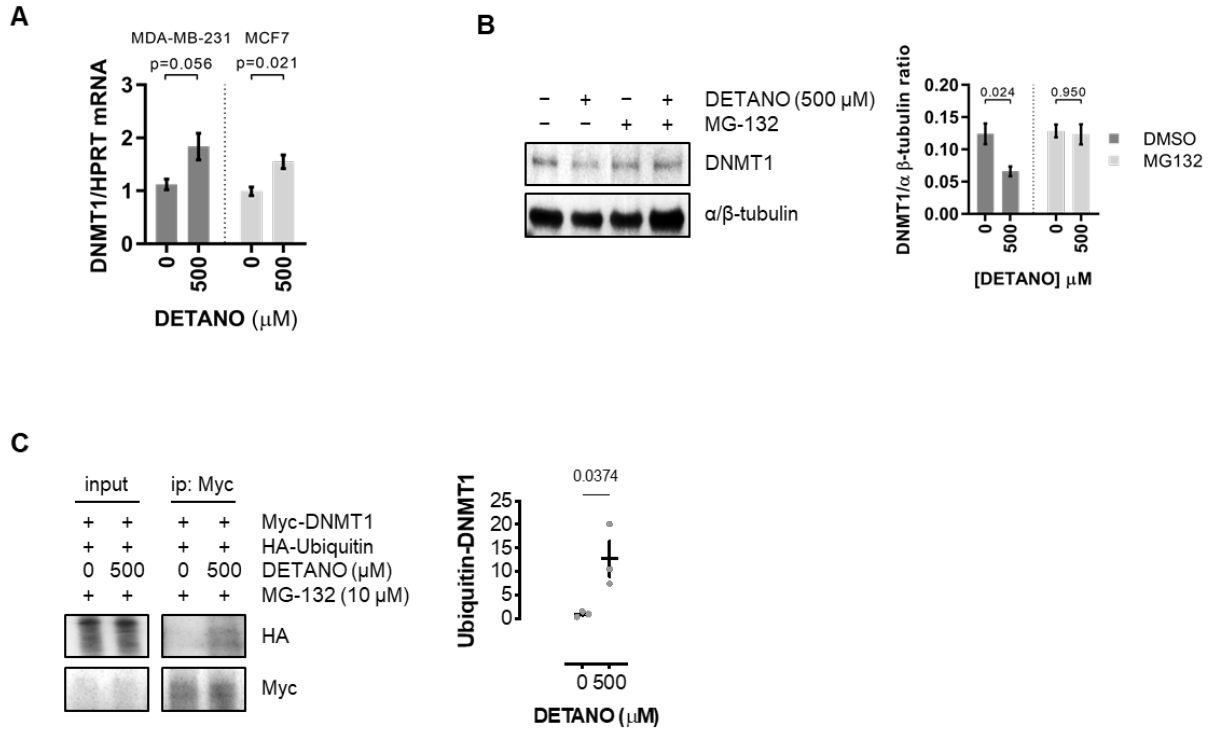
Fig. S3. SNO signaling induces DNMT1 protein degradation.
A Relative DNMT1 mRNA expression in MDA-MB-231 and MCF7 cells cultured with DETANO or vehicle for 48 hours. Graph shows mean expression (±sem; n = 3) and significance was calculated by two-tailed, unpaired t test. **B** Immunoblot and graph showing relative DNMT1 expression in MDA-MB-231 cells treated with DETANO and/or MG-132 (10 µM) compared to vehicle control. Graph shows mean expression (±sem; n = 4) and significance was calculated by two-way ANOVA with Sidak multiple comparisons test. **C** Immunoblots of input and Myc-tag immunoprecipitated lysates from HEK293 cells expressing Myc-DNMT1 and HA-Ubiquitin and treated with vehicle or DETANO and MG132. Graph shows mean HA normalized to Myc intensities (±sem; n = 3) and significance was calculated by two-tailed, unpaired t test.
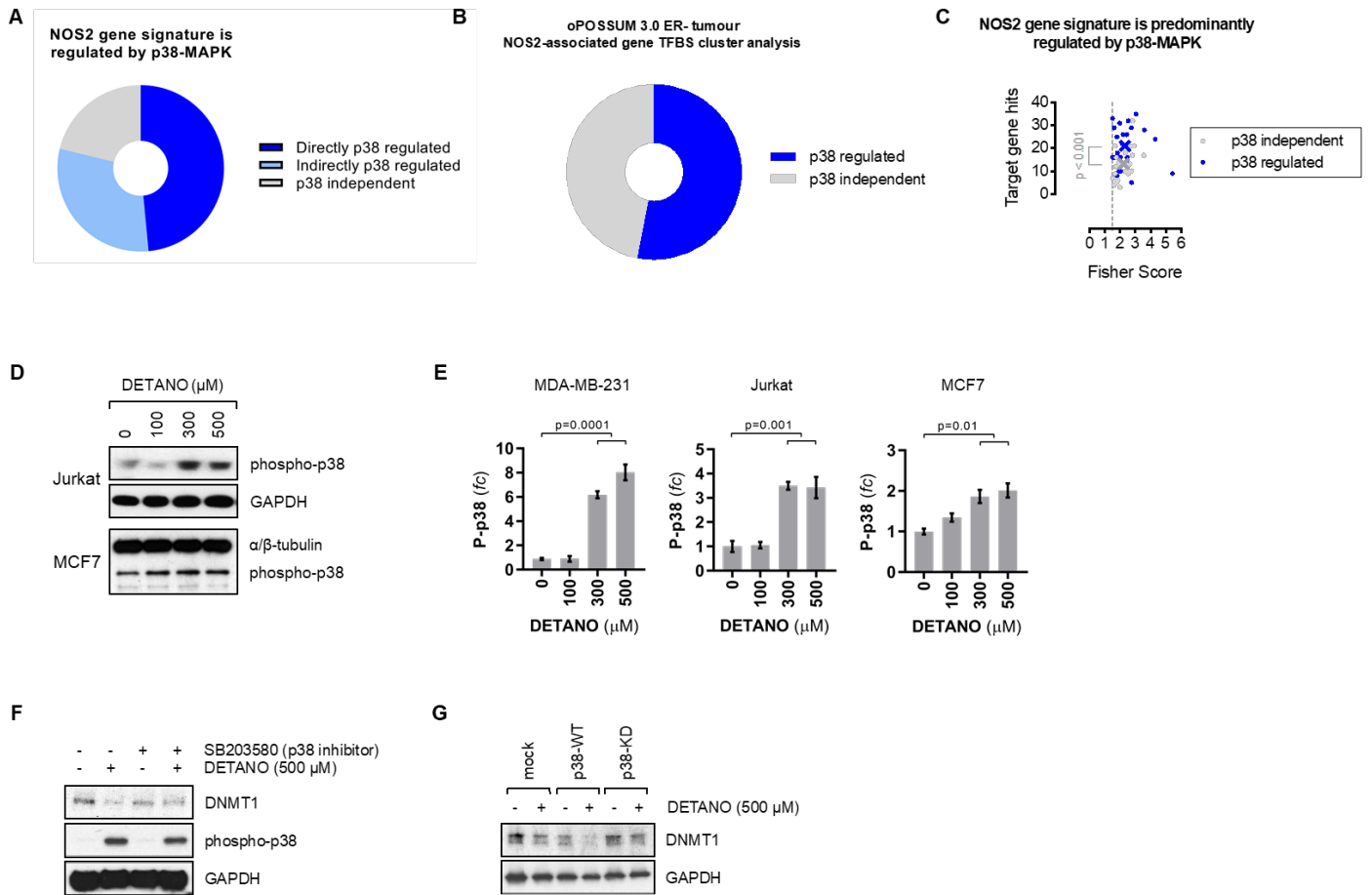
Fig. S4. p38-MAPK mediates NOS2-induced DNMT1 degradation.
A Graph depicting the relative number of NOS2-associated upregulated genes (Additional File 1, Supplementary Table S4) that are either directly or indirectly controlled by p38-MAPK activity identified from the TRANSFAC database (Additional File 1, Supplementary Table S5). **B** Graph depicting the relative number of NOS2-associated upregulated genes (Additional File 1, Supplementary Table S4) that are controlled by p38-MAPK activity identified from the oPOSSUM database (Additional File 1, Supplementary Table S6). **C** Relative contribution of p38-regulated compared to p38-independent transcription factors in the NOS2-associated gene signature. The graph depicts Fisher score compared to the number of gene hits from oPOSSUM transcription factor cluster analysis grouped into p38-independent (grey) and p38-regulated (blue) transcription factor families. X represent the mean of each group and statistical difference between the means was calculated by unpaired, two-tailed t test. **D** Immunoblots of relative phospho-p38 (Thr180/Tyr182) expression in Jurkat and MCF7 cells cultured with DETANO for 48 hours. **E** Densitometric analyses of phospho-p38 (Thr180/Tyr182) expression in human cell lines cultured with DETANO for 48 hours. Data shows mean normalized phospho-p38 expression as fold change of controls (±sem; n = 3-6). Significance was calculated by one-way ANOVA with Dunnett's multiple comparisons test. **F** Immunoblots of relative DNMT1 and phospho-p38 (Thr180/Tyr182) expression in MDA-MB-231 cells cultured for 24 hours with or without DETANO or 10 µM SB203580 (p38 inhibitor). **G** Immunoblot of relative DNMT1 expression in vehicle- or DETANO-treated HEK293 cells expressing wild-type or inactive p38a and compared to mock transfected cells.
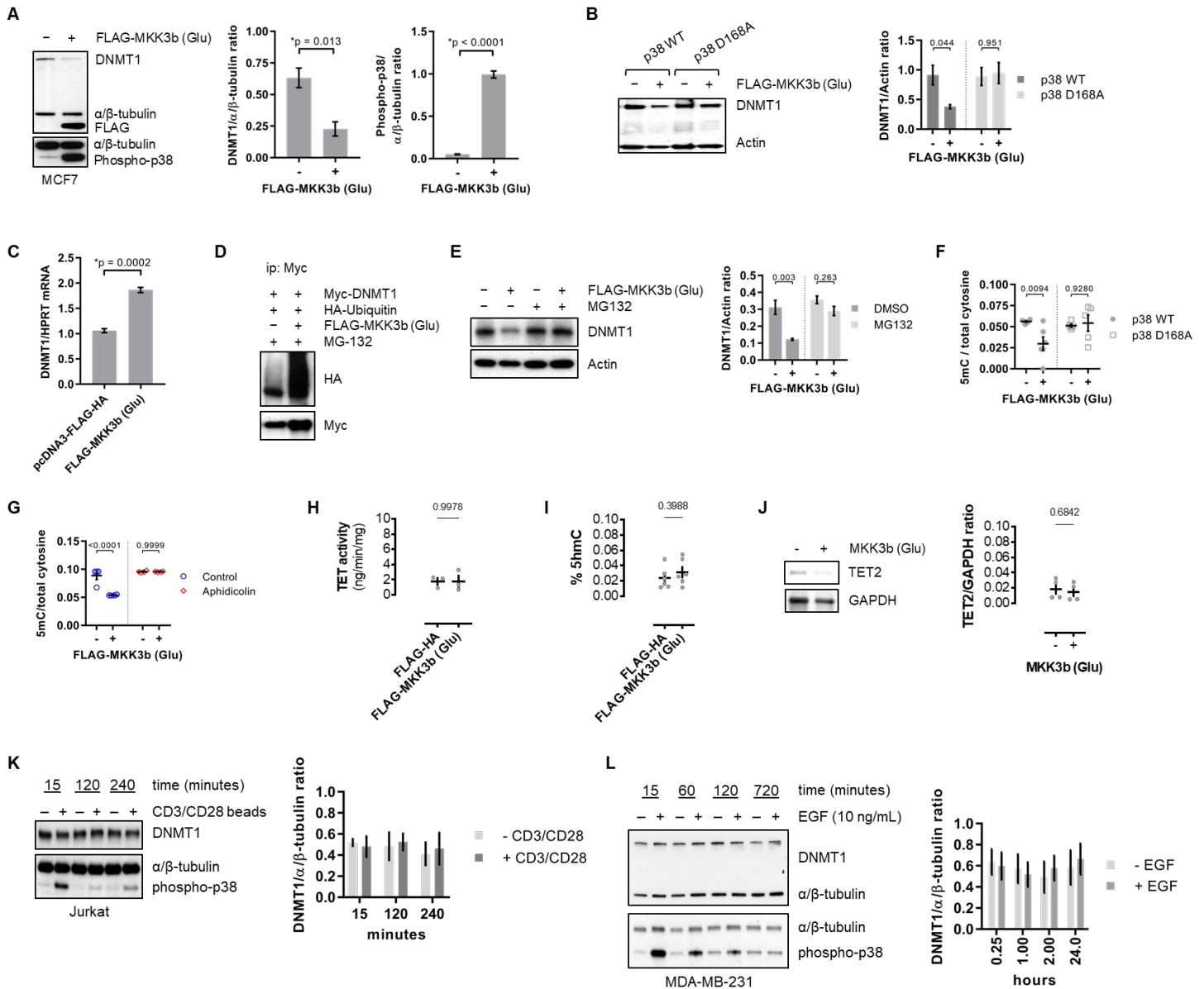
Fig. S5. Direct p38 activation induces passive demethylation.
A Immunoblot of relative DNMT1, phospho-p38 and FLAG-tag expression in MCF7 cells transfected with control or FLAG-MKK3b (Glu) plasmids. Graphs depict mean normalized DNMT1 and phospho-p38 expression (±sem; n = 3) and significance was calculated by two-tailed, unpaired t test. **B** Immunoblot of relative DNMT1 expression in HEK293 cells co-transfected with either control or FLAG-MKK3b (Glu) plasmids and either wild-type or inactive p38. Graph shows mean normalized DNMT1 expression (±sem; n = 3) and significance was calculated by two-way ANOVA with Sidak's multiple comparisons test. **C** Relative DNMT1 mRNA expression in HEK293 cells transfected with control or MKK3b (Glu) plasmids. Graph depicts mean expression values (±sem; n = 3). Significance was calculated by two-tailed, unpaired t test. **D** Immunoblots showing DNMT1 ubiquitination in control or MKK3b (Glu) expressing HEK293 cells. Cells were co-transfected with Myc-DNMT1, HA-ubiquitin and either control or FLAG-MKK3b (Glu) and incubated with MG132 for 3 hours. **E** Immunoblot of relative DNMT1 expression in control or MKK3b (Glu) expressing HEK293 cells treated with vehicle or MG132 for 3 hours. Graph shows mean normalized DNMT1

7

expression (±sem; n = 3) and significance was calculated by two-way ANOVA with Sidak's multiple comparisons test. **F** 5-methylcytosine content from HEK293 cells co-transfected with control or MKK3b (Glu) and wild-type or inactive mutant p38 expression plasmids. Graph shows mean values (±sem; n = 6) and significance was calculated by two-way ANOVA with Sidak's multiple comparisons test. **G** 5-methylcytosine content from HEK293 cells transfected with either control or MKK3b (Glu) plasmids and incubated with or without aphidicolin. Graph shows mean values (±sem; n = 6) and significance was calculated by two-way ANOVA with Sidak's multiple comparisons test. **H** TET enzymatic activity from cells transfected with control or MKK3b (Glu) plasmids. Graph shows mean activity (±sem; n = 3) and significance was calculated by two-tailed, unpaired t test. **I** 5-hydroxymethylcytosine content from HEK293 cells transfected with either control or MKK3b (Glu) plasmids. Graph shows mean activity (±sem; n = 6) and significance was calculated by two-tailed, unpaired t test. **J** Immunoblot of TET2 expression in HEK293 cells transfected with either control or MKK3b (Glu) plasmids. Graph shows mean expression (±sem; n = 4) and significance was calculated by two-tailed, unpaired t test. **K** Immunoblot of relative DNMT1 and phospho-p38 (Thr180/Tyr182) expression in Jurkat cells stimulated with CD3/CD28 beads for the indicated times. Graph shows mean normalized DNMT1 expression (±sem; n = 3). **L** Immunoblot of relative DNMT1 and phospho-p38 (Thr180/Tyr182) expression in MDA-MB-231 cells stimulated with recombinant human EGF for the indicated times. Graph shows mean normalized DNMT1 expression (±sem; n = 3).
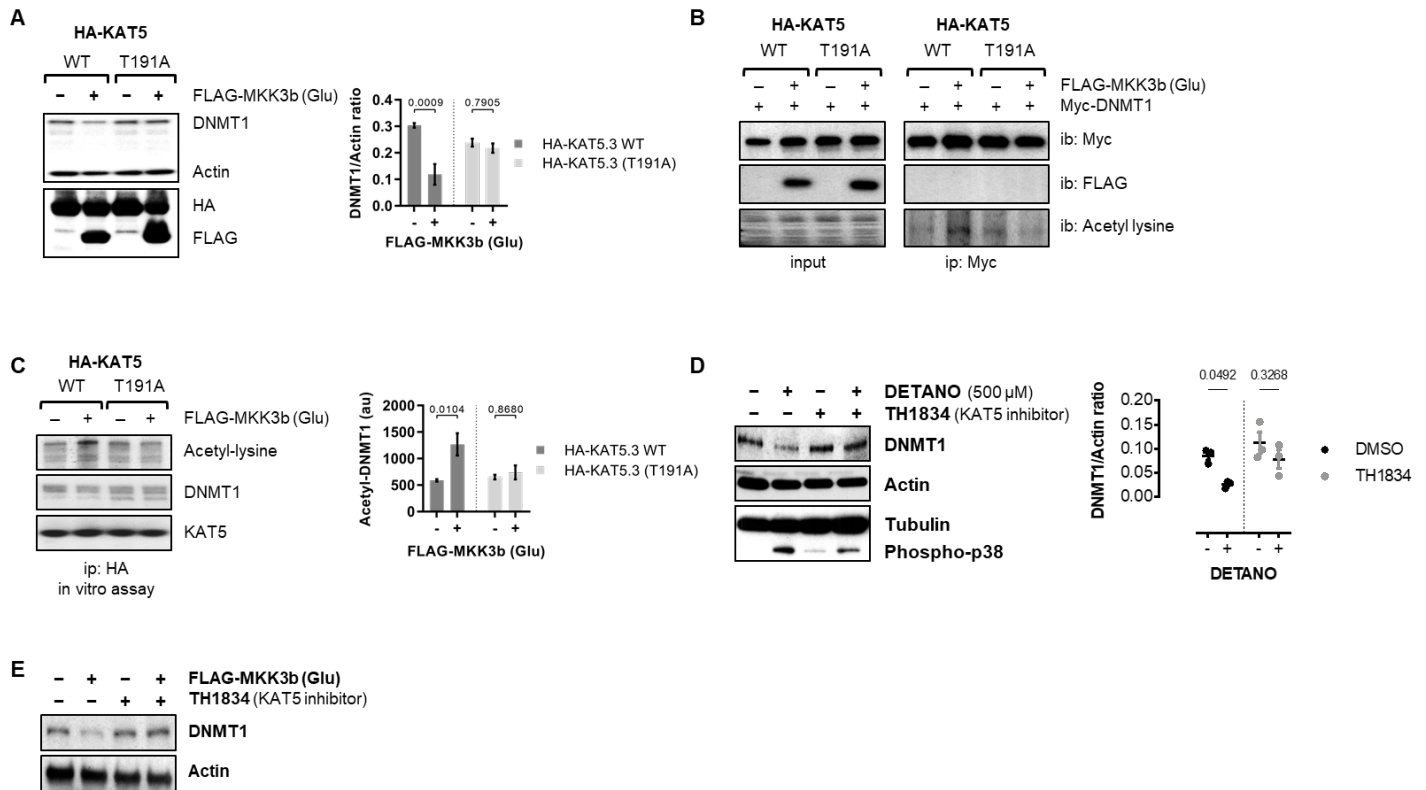
Fig. S6. p38 signaling induces passive DNA demethylation via KAT5 activation.
A Immunoblot showing relative DNMT1 protein and FLAG- and HA-epitope expression in HEK293 cells co-transfected with either WT or T191A HA-KAT5 and control or FLAG-MKK3b (Glu) plasmids. Graph shows mean normalized DNMT1 expression (±sem; n = 3) and significance was calculated by two-way ANOVA with Sidak's multiple comparisons test. **B** Immunoblots of Myc-DNMT1, FLAG and acetyl-lysine from input and Myc-tag immunoprecipitated lysate from HEK293 cells co-expressing Myc-DNMT1 and either HA-KAT5 WT or HA-KAT5 (T191A) and control or FLAG-MKK3b (Glu) plasmids. **C** DNMT1 acetyl-lysine formation in an in vitro acetyltransferase activity assay using HA-immunoprecipitated KAT5 from WT or T191A expressing cells which have been co-transfected with either control or FLAG-MKK3b (Glu) plasmids. Densitometric analysis shows mean acetylation (±sem; n = 3) and significance was determined by two-way ANOVA with Sidak's multiple comparisons test. **D** DNMT1 protein expression in MDA-MB-231 cells treated with vehicle or DETANO and cultured with the KAT5-specific inhibitor TH1834 (50 μM) or vehicle. Graph shows normalized mean densitometric values (±sem; n = 3) and significance was determined by two-way ANOVA with Sidak's multiple comparisons test. **E** DNMT1 protein expression in MCF7 cells transfected with either control or FLAG-MKK3b (Glu) plasmids and treated with vehicle or TH1834.

9
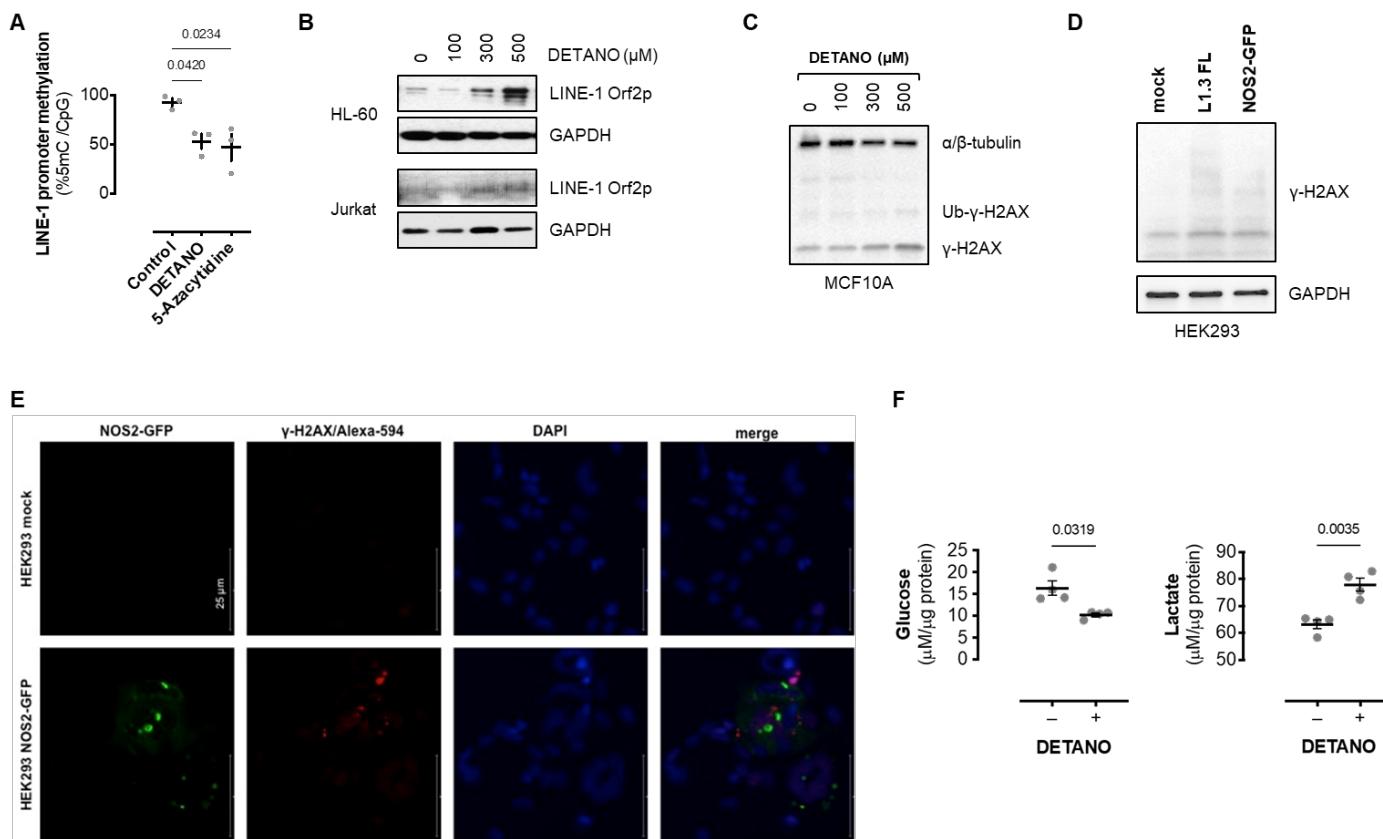
Fig. S7. NOS2 induces LINE-1 expression and DNA damage.
A LINE-1 promoter methylation in MDA-MB-231 cells treated with DETANO (300 µM) or 5-azacytidine (1 µM) for 48 hours. Data shown represent the mean % 5-mC associated per CpG cytosine residues (±sem; n=3). Significance was calculated by one-way ANOVA with Dunnett's multiple comparisons test. **B** Immunoblots of relative LINE-1 Orf2p expression from HL-60 or Jurkat cell lines cultured with DETANO or vehicle for 48 hours. **C** Immunoblot of relative γ-H2AX expression from MCF10A cells cultured with DETANO or vehicle for 48 hours. **D** Immunoblot of relative γ-H2AX expression from HEK293 cells 48 hours after transfection with either full-length human L1.3 element or NOS2-GFP plasmids. **E** Immunofluorescent images of formalin-fixed HEK293 cells that have been mock or NOS2-GFP transfected. NOS2 and γ-H2AX expression are displayed individually and merged with DAPI counterstain. Images recorded at 20X magnification and white bar represents 25 µm. **F** Graphs showing mean glucose and lactate in culture media from MCF10A control or NO-transformed cells after 96 hours in culture. Data shown are mean normalized concentrations (±sem; n=4) and significance calculated by unpaired, two-way *t* test.

Table S1. Promoter methylation of NOS2-associated genes.

Table S1. Promoter methylation of NOS2-associated genes

GenBank ID	Gene Symbol	Fold Change	p value	TSS CGI (UCSC hg38)
AL569511	KRT6A/B/C/E	52.7	0.002	−
J00269	KRT6A/C/E	42.1	0.002	−
NM_021804	ACE2	17	0.005	−
L42612	KRT6B	15.9	0.001	−
AI831452	KRT6B	14.3	<0.001	−
NM_025087	FLJ21511	12.2	0.001	+
NM_000422	KRT17	8.6	0.009	−
Z19574	KRT17	8.3	0.005	−
NM_000584	IL8	6.8	0.003	−
NM_003064	SLPI	6	0.001	−
NM_018004	TMEM45A	5.6	0.001	+
NM_002964	S100A8	5	0.01	−
L25541	LAMB3	4.9	0.002	−
NM_001793	CDH3	4.3	0.005	+
AB018009	SLC7A5	4.2	0.008	+
NM_018455	C16orf60	4.1	0.002	+
X57348	SFN	4	0.001	+
NM_001630	ANXA8	3.9	0.006	+
NM_005629	SLC6A8	3.9	0.006	+
NM_012101	TRIM29	3.8	0.002	+
NM_002061	GCLM	3.4	<0.001	+
AF132818	KLF5	3.4	<0.001	+
NM_022121	PERP	3.4	0.003	+
NM_003878	GGH	3.2	0.004	+
NM_007196	KLK8	3.2	0.002	+
NM_016593	CYP39A1	3.1	0.01	+
NM_003662	PIR	3	0.002	+
NM_001047	SRD5A1	2.9	0.003	+
X57348	SFN	2.8	0.005	+
NM_005342	HMGB3	2.8	0.002	+
NM_006623	PHGDH	2.7	0.002	+
AV712602	PTPLB	2.6	<0.001	+
X16447	CD59	2.5	0.001	+
NM_003392	WNT5A	2.4	0.002	+
NM_000611	CD59	2.4	0.002	+
BE964473	RPE	2.3	0.001	+
NM_000050	ASS	2.3	0.008	+
NM_002633	PGM1	2.1	0.003	+
D84454	SLC35A2	2.1	0.002	+
BF116254	TPI1	2	0.001	+
NM_005333	HCCS	2	0.001	+
NM_001428	ENO1	2	<0.001	+
NM_000610	CD44	2	0.003	+
BF939365	CALU	1.9	0.002	+
NM_014637	MTFR1	1.9	0.004	+
NM_000365	TPI1	1.9	0.002	+
AF289489	ASPH	1.9	0.006	+
BC003375	MRPL3	1.8	0.002	+
AI186712	PPP1CB	1.7	<0.001	+

Table S2. Patient metadata.

	Tumor NOS2		
	Low	High	p value[1]
n	10	43	
Ethnicity			
WestAfrican	0.446	0.398	0.756
NativeAm	0.016	0.003	0.419
European	0.538	0.599	0.704
Age	54.4	52.7	0.817
Education[2]	1	1	0.912
Income[2]	1.2	1	0.415
Smoking (pack years)	17.1	14.2	0.797
BMI rank[2]	1.5	0.976	0.061
Survival (months)	67.5	54.8	0.48
Tumour stage	1.4	1.14	0.179
ER expression[3]	0.7	0.45	0.17

[1] p value calculated from two-tailed heteroscedastic t test
[2] Rankings are described in Terunuma A, et al. The Journal of Clinical Investigation 2014, 124(1):398-412.
[3] ER-positive = 1; ER-negative = 0

Table S3. TRANSFAC analysis: ER-negative NOS2 gene signature.

Gene set	Gene set name	score	p value	FDR	
188	V$AML1_01	0.3401	0.0067	0.5486	
377	V$COREBINDINGFACTOR_	0.4361	0.0067	0.5486	
135	V$CEBP_Q2	0.216	0.0133	0.5486	
557	RACCACAR_V$AML_Q6	0.3732	0.0133	0.5486	
268	V$STAT5A_01	0.2414	0.0167	0.5486	
409	V$AML_Q6	0.3472	0.0167	0.5486	Directly p38 regulated
269	V$STAT5B_01	0.283	0.02	0.5486	
339	V$HOXA4_Q2	0.1717	0.02	0.5486	
611	TTCYNRGAA_V$STAT5B_0	0.1958	0.0233	0.6109	
162	V$STAT3_01	0.6984	0.03	0.6912	
213	V$ETS1_B	0.2795	0.03	0.6912	
344	V$MAF_Q6	0.2	0.03	0.6912	
411	V$ETS_Q4	0.3525	0.04	0.7131	
206	V$NFAT_Q6	0.1804	0.0433	0.7131	
72	V$CEBPB_01	0.2123	0	0	
444	V$CEBP_Q2_01	0.2201	0.04	0.7131	
121	V$AP1_Q6	0.1654	0.0033	0.5486	
400	V$AML1_Q6	0.3401	0.0067	0.5486	
214	V$ETS2_B	0.3049	0.01	0.5486	
140	V$NFKB_Q6	0.329	0.0133	0.5486	
120	V$AP1_Q2	0.1708	0.04	0.7131	Indirectly p38-regulated
396	V$ELF1_Q6	0.4535	0.01	0.5486	
170	V$NKX25_02	0.2429	0.0133	0.5486	
603	RGAGGAARY_V$PU1_Q6	0.3258	0.0133	0.5486	
352	V$PU1_Q6	0.3953	0.02	0.5486	
397	V$IRF1_Q6	0.2665	0.02	0.5486	
384	V$OSF2_Q6	0.1809	0.0133	0.5486	
202	V$FREAC4_01	0.2742	0.0167	0.5486	
224	V$MSX1_01	0.2091	0.0167	0.5486	
320	V$RP58_01	0.2973	0.0367	0.7131	p38-independent
104	V$BRN2_01	0.1719	0.04	0.7131	
275	V$POU6F1_01 (BRN5)	0.2099	0.0433	0.7131	
385	V$SMAD4_Q6	0.112	0.0467	0.7467	

Table S4. NOS2-associated gene expression oPOSSUM transcription factor analysis.

TFBS Cluster ID	Class	Family	Target gene hits	Target gene non-hits	Target cluster hits	Target cluster nucleotide rate	Z-score	Fisher score	Members*	Consensus LINE-1 5'-UTR (ref)
c109	Helix-Turn-Helix	Myb	9	30	11	0.00296	12.487	5.446	Myb_1 Mybl1	
c16	Ig-fold	Stat	24	15	51	0.00975	1.975	4.321	Stat3 STAT1	
c87	Zinc-coordinating	BetaBetaAlpha-zinc finger	28	11	121	0.0192	1.673	3.596	Gfi	
c68	Zinc-coordinating	BetaBetaAlpha-zinc finger	17	22	33	0.00837	7.295	3.58	Gm397_2 Zscan4_2	
c55	Winged Helix-Turn-Helix	Ets	35	4	563	0.0797	0.927	3.054	SPIB SPI1 FEV Elp74EF GABPA ELK4 ELK1 ETS1 ELF5	
c88	Zinc-coordinating	BetaBetaAlpha-zinc finger	21	18	66	0.0146	3.813	2.92	Zfx	
c70	Zinc-coordinating	BetaBetaAlpha-zinc finger	32	7	319	0.0323	4.892	2.825	Zfp410_1 YY1	
c95	Zinc-coordinating	BetaBetaAlpha-zinc finger	17	22	40	0.00761	5.598	2.811	INSM1	
c149	Zipper-type	Leucine Zipper	10	29	11	0.00261	0.77	2.762	MafK_2	
c150	Zipper-type	Leucine Zipper	5	34	5	0.00127	5.708	2.759	Jundm2_1 Atf1_1	
c127	Winged Helix-Turn-Helix	Ets	29	10	124	0.0278	-5	2.744	Elf3_1 Elf_1 Sfpi1_1 Ehf_2 Gabpa_1 Spdef_1 Spdef_2	
c167	Helix-Turn-Helix	Homeo	13	26	24	0.00533	4.519	2.628	Hoxa3_1	
c143	Zipper-type	Helix-Loop-Helix	21	18	48	0.00913	-0.127	2.628	Myf	
c72	Zinc-coordinating	BetaBetaAlpha-zinc finger	32	7	349	0.0347	6.104	2.53	ZEB1 Zbtb7b_2	
c46	Beta-Hairpin-Ribbon	T	9	30	14	0.00301	5.959	2.52	Eomes_1 T	
c60	Zinc-coordinating	Glial Cells Missing (GCM)	10	29	13	0.0033	3.967	2.517	Gcm1_1	
c8	Zipper-type	Leucine Zipper	13	26	24	0.00456	5.776	2.513	Cebpa	
c34	Zinc-coordinating	BetaBetaAlpha-zinc finger	16	23	33	0.00837	3.826	2.467	Egr1_2	
c108	Helix-Turn-Helix	Myb	26	13	113	0.0143	2.892	2.446	Myb	
c26	Zinc-coordinating	MH1	13	26	23	0.0062	6.844	2.426	Smad3_1	
c27	Zinc-coordinating	BetaBetaAlpha-zinc finger	18	21	38	0.00964	1.994	2.372	Osr1_2 Osr2_2 Osr1_1 Osr2_1	
c58	Other Alpha-Helix	MADS	10	29	12	0.00266	1.039	2.353	Srf_1	
c9	Zipper-type	Leucine Zipper	26	13	147	0.0225	5.251	2.185	CEBPA HLF NFIL3	
c50	Zipper-type	Helix-Loop-Helix	22	17	60	0.0158	0.9	2.138	Max_1 Bhlhb2_1 Max_2 Tcfe2a_1 Ascl2_1 Myf6_1 Tcfe2a_2 Bhlhb2_2	
c151	Zipper-type	Leucine Zipper	10	29	14	0.00355	3.903	2.057	Jundm2_2	
c28	Zinc-coordinating	BetaBetaAlpha-zinc finger	16	23	30	0.00791	-2.151	2.021	Egr1_1 Sp4_1 Bcl6b_2	
c31	Zinc-coordinating	BetaBetaAlpha-zinc finger	3	36	4	0.00108	8.029	2.001	Plagl1_2	
c64	Other	Other	14	25	28	0.00488	4.255	1.975	Spz1	1
c41	Other Alpha-Helix	High Mobility Group	31	8	328	0.0511	1.167	1.967	SOX9 Sox_30_1 Sox5 SRY SOX10 SOX2 SOX17	
c38	Zinc-coordinating	BetaBetaAlpha-zinc finger	13	26	22	0.00558	2.673	1.935	Hic1_2	
c5	Helix-Turn-Helix	Arid	10	29	12	0.00323	-2.192	1.924	Arid3a_1	
c59	Zinc-coordinating	Glial Cells Missing (GCM)	6	33	8	0.00216	4.94	1.847	Gcm1_2	
c160	Other Alpha-Helix	High Mobility Group	17	22	37	0.00908	-3.993	1.836	Sox1_1 Sox8_2 Hbp1_1	1
c10	Zipper-type	Leucine Zipper	18	21	32	0.00406	-1.247	1.835	CREB1	
c110	Helix-Turn-Helix	Myb	8	31	12	0.003	5.425	1.805	Myb_2 Mybl1_2	
c24	Ig-fold	Runt	25	14	118	0.0206	5.029	1.803	RUNX1-3	2
c104	Zinc-coordinating	BetaBetaAlpha-zinc finger	25	14	156	0.0249	0.371	1.793	Klf4	
c102	Zinc-coordinating	BetaBetaAlpha-zinc finger	5	34	5	0.00119	1.634	1.772	Zbtb12_2	
c61	Winged Helix-Turn-Helix	E2F	16	23	40	0.00507	4.616	1.742	E2F1	
c138	Zipper-type	Helix-Loop-Helix	12	27	18	0.00342	0.546	1.709	NHLH1	
c119	Helix-Turn-Helix	Homeo	9	30	16	0.00304	4.413	1.675	PBX1	
c142	Zipper-type	Helix-Loop-Helix	21	18	86	0.0136	6.662	1.66	EBF1	
c128	Ig-fold	Rel	29	10	230	0.0294	0.497	1.616	NFATC2 REL RELA NF-kappaB NFKB1	
c11	Zipper-type	Leucine Zipper	29	10	215	0.0253	2.357	1.611	NFE2L1::MafG NFE2L2 AP1 NFE2L2	
c29	Zinc-coordinating	BetaBetaAlpha-zinc finger	16	23	39	0.00986	3.338	1.608	Klf7_1 Sp4_2	
c86	Zinc-coordinating	BetaBetaAlpha-zinc finger	4	35	5	0.00111	3.716	1.608	Zfp187_1	
c37	Zinc-coordinating	BetaBetaAlpha-zinc finger	7	32	13	0.0033	8.309	1.522	Hic1_1	
c134	Winged Helix-Turn-Helix	IRF	16	23	35	0.00804	0.327	1.518	Irf3_1 Irf4_1 Irf5_1 Irf6_1 Isgf3g_1	
c113	Helix-Turn-Helix	Homeo	33	6	715	0.097	2.34	1.509	Prrx2 Pdx1 Lhx3 Nobox Nkx2-5 HOXA5 HNF1B HNF1A	3

* p38-regulated highlighted

14

References:
1. Tchénio T, et al., Nucleic Acids Res. 2000 Jan 15;28(2):411-5. doi: 10.1093/nar/28.2.411.
2. Yang N, et al., Nucleic Acids Res. 2003 Aug 15;31(16):4929-40. doi: 10.1093/nar/gkg663.
3. Penzkofer T, et al., Nucleic Acids Res. 2017 Jan 4;45(D1):D68-D73. doi: 10.1093/nar/gkw925. Epub 2016 Oct 18.

Table S5. Antibodies used in this study.

Table S5. Antibodies used in this study

	Supplier	Cat #	Fold dilution
Primary antibodies:			
Acetyl-lysine	Cell Signaling	9441	1000
ALDH1A3	Abcam	ab129815	1000
CD44	Cell Signaling	3570	1000
DNMT1	Cell Signaling	5032	1000
ERK1/2	Cell Signaling	4695	1000
FLAG	Sigma	F1804	5000
GAPDH	Cell Signaling	2118	3000
GFP	Cell Signaling	2955	1000
HA-tag	Thermo Scientific	26183	2000
histone H2A.X (phospho S139)	Cell Signaling	9718	2000
KAT5	Novus	NBP2-20647	1000
LINE-1 Orf2p	Abcam	ab106004	500
Myc-tag	Cell Signaling	2276	2000
NOS2	Cell Signaling	13120	1000
Notch1	Cell Signaling	4380	1000
p38-MAPK (phospho T180/Y182)	Cell Signaling	9215	1000
TET2	Cell Signaling	45010	1000
total p38	Cell Signaling	8690	1000
α/β-tubulin	Cell Signaling	2148	3000
β-actin	Sigma	A5316	10000
Secondary antibodies:			
anti-chicken	InVitrogen	A16054	2000
anti-mouse IgG (H+L) Alexa Fluor 488	InVitrogen	A11008	10000
anti-mouse IgG-HRP	Cell Signaling	7076	5000
anti-rabbit IgG-HRP	Cell Signaling	7074	5000
streptavidin-HRP	Cell Signaling	3999	10000
FACS antibodies:			
DNMT1-PE	Cell Signaling	64503	500
Rabbit IgG-PE	Cell Signaling	5742	3000
Immunofluorescence antibodies:			
histone H2A.X (phospho S139)	Cell Signaling	9718	500
anti-rabbit IgG (H+L) Alexa Fluor 594	InVitrogen	A11021	5000
Immunoprecipitation antibodies:			
anti-HA-tag conjugated magnetic beads	Cell Signaling	11846	*n/a*
anti-Myc-tag conjugated magnetic beads	Cell Signaling	5698	*n/a*

Table S6. qPCR primers.

Table S6. qPCR primers

Gene	UPL probe	Right/Forward Primer	Left/Reverse Primer
DNMT1	9	ACG GGA CTG GAC AGC TTG	ACC AAG AAC GGC ATC CTG TA
HPRT	22	GTG TCA ATT ATA TCT TCC ACA ATC AAG	GAC CAG TCA ACA GGG GAC AT
hL1-ORF2	–	GAG AGG ATG CGG AGA AAT AGG A	GGA TGG CTG GGT CAA ATG GT

Dataset S1 (separate file). Differentially methylated loci (beta ≥ 0.2) MDA-MB-231 control 5AZA DETANO

SI References

1. Terunuma A, Putluri N, Mishra P, Mathé EA, Dorsey TH, Yi M, Wallace TA, Issaq HJ, Zhou M, Killian JK, Stevenson HS, Karoly ED, Chan K, Samanta S, Prieto D, Hsu TY, Kurley SJ, Putluri V, Sonavane R, Edelman DC, Wulff J, Starks AM, Yang Y, Kittles RA, Yfantis HG, Lee DH, Ioffe OB, Schiff R, Stephens RM, Meltzer PS, Veenstra TD, Westbrook TF, Sreekumar A, Ambs S. MYC-driven accumulation of 2-hydroxyglutarate is associated with breast cancer prognosis. J Clin Invest. 2014 Jan;124(1):398-412. doi: 10.1172/JCI71180. Epub 2013 Dec 9. PMID: 24316975; PMCID: PMC3871244.
2. Tchénio T, Casella JF, Heidmann T. Members of the SRY family regulate the human LINE retrotransposons. Nucleic Acids Res. 2000 Jan 15;28(2):411-5. doi: 10.1093/nar/28.2.411. PMID: 10606637; PMCID: PMC102531.
3. Yang N, Zhang L, Zhang Y, Kazazian HH Jr. An important role for RUNX3 in human L1 transcription and retrotransposition. Nucleic Acids Res. 2003 Aug 15;31(16):4929-40. doi: 10.1093/nar/gkg663. PMID: 12907736; PMCID: PMC169909.
4. Penzkofer T, Jäger M, Figlerowicz M, Badge R, Mundlos S, Robinson PN, Zemojtel T. L1Base 2: more retrotransposition-active LINE-1s, more mammalian genomes. Nucleic Acids Res. 2017 Jan 4;45(D1):D68-D73. doi: 10.1093/nar/gkw925. Epub 2016 Oct 18. PMID: 27924012; PMCID: PMC5210629.